Final Report

A PRELIMINARY DESIGN STUDY OF A MICROPARTICLE ACCELERATOR

April 14, 1964 to July 6, 1964

Contract NAS2-1873 S/A No. 1

Prepared for:

Ames Research Center

National Aeronautics and Space Administration

Moffett Field, California

ION PHYSICS CORPORATION

Burlington, Massachusetts

[redacted]

FOREWORD

This final report was prepared by those members of the staff of the Particle Physics and Electro-Physics Departments of Ion Physics Corporation involved in "A Design Study for Microparticle Accelerator" under NASA Contract NAS2-1873 S/A No. 1. The work was administered through the Planetary Science Branch of the Ames Research Center, Moffett Field, California. The technical monitor was James F. Vedder.

Principal contributors to the execution of the study and preparation of this report were:

Dr. K. W. Arnold

R. N. Cheever

Dr. A. S. Denholm

R. E. Elcox

J. E. Lavelle

S. C. Zanon

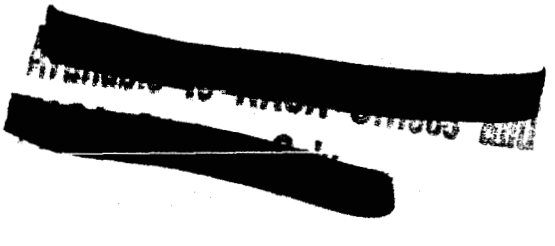

ABSTRACT

Design considerations, drawings, and circuit diagrams for a single stage prototype microparticle accelerator are presented. Qualification tests are also described which will assess the reliability of the system and its components and confirm that they operate according to specifications. The specifications for the design are generally those outlined in the document "Design Requirements; A Design Study for Microparticle Accelerator," dated March 31, 1964 as prepared by Ion Physics Corporation under Contract NAS2-1873.

TABLE OF CONTENTS

LIST OF ILLUSTRATIONS

1. INTRODUCTION

Detailed design of components for a single-stage prototype microparticle accelerator has been accomplished. Port modifications have also been designed to allow the mounting of the prototype system in an existing four-foot-diameter stainless steel vacuum vessel closely simulating the anticipated containing vessel.

For purposes of reference, a layout of the entire bushing-generator-switch package is given in Drawing No. S23052. With but few exceptions, the components have been designed to the specifications outlined in the document "Design Requirements, A Design Study for Microparticle Accelerator," dated March 31, 1964, as prepared by Ion Physics Corporation under Contract NAS2-1873. These exceptions, involving the bushing and the electronics circuitry, are duly noted and have been made either to improve performance or to simplify the design with no sacrifice of performance.

2. ELECTROSTATIC GENERATOR

The prototype Van de Graaff type electrostatic generator is detailed in the drawings numbered 23004 through 23020, 23023 through 23046, 23050, 23051, and 23053 through 23057. The design as shown incorporates a 3.5-inch wide charging belt driven by a 1.8 hp, 400 cycle, 3-phase electric motor. This configuration should be capable of generating over 750 kV at over 200 μA current. There is thus a generous reserve capacity for future expansion of the accelerator. This capacity is not needed at present, however, so the machines to be assembled will use 2-inch belts and 1/3 hp, 60-cycle, 3-phase motors of approximately the same physical size. This combination ought to provide over 100 μA current at over 600 kV, which is more than adequate, and will not require the use of a 60-400 cycle converter. The generator is essentially a scaled-down version of those marketed commercially by the High Voltage Engineering Corporation in their particle accelerators. These machines have an impressive record for durability and reliability and this new design should share in these attributes.

The electrical circuit for the generator is shown in Fig. 1. Voltage control and stabilization is effected in a time proved manner. The generator structure is electrostatically graded by a series connected stack of precision resistors (type BFT, Resistance Products Corporation). The current in this stack is proportional to terminal voltage and can be used to indicate this quantity on an appropriately calibrated microammeter. This same current can be used to supply a control signal to the grid of a 6BK4 high voltage triode which, in turn, adjusts the potential of the corona points charging the belt. A feedback loop is thus established by which the generator becomes self-regulating against voltage variations which might occur

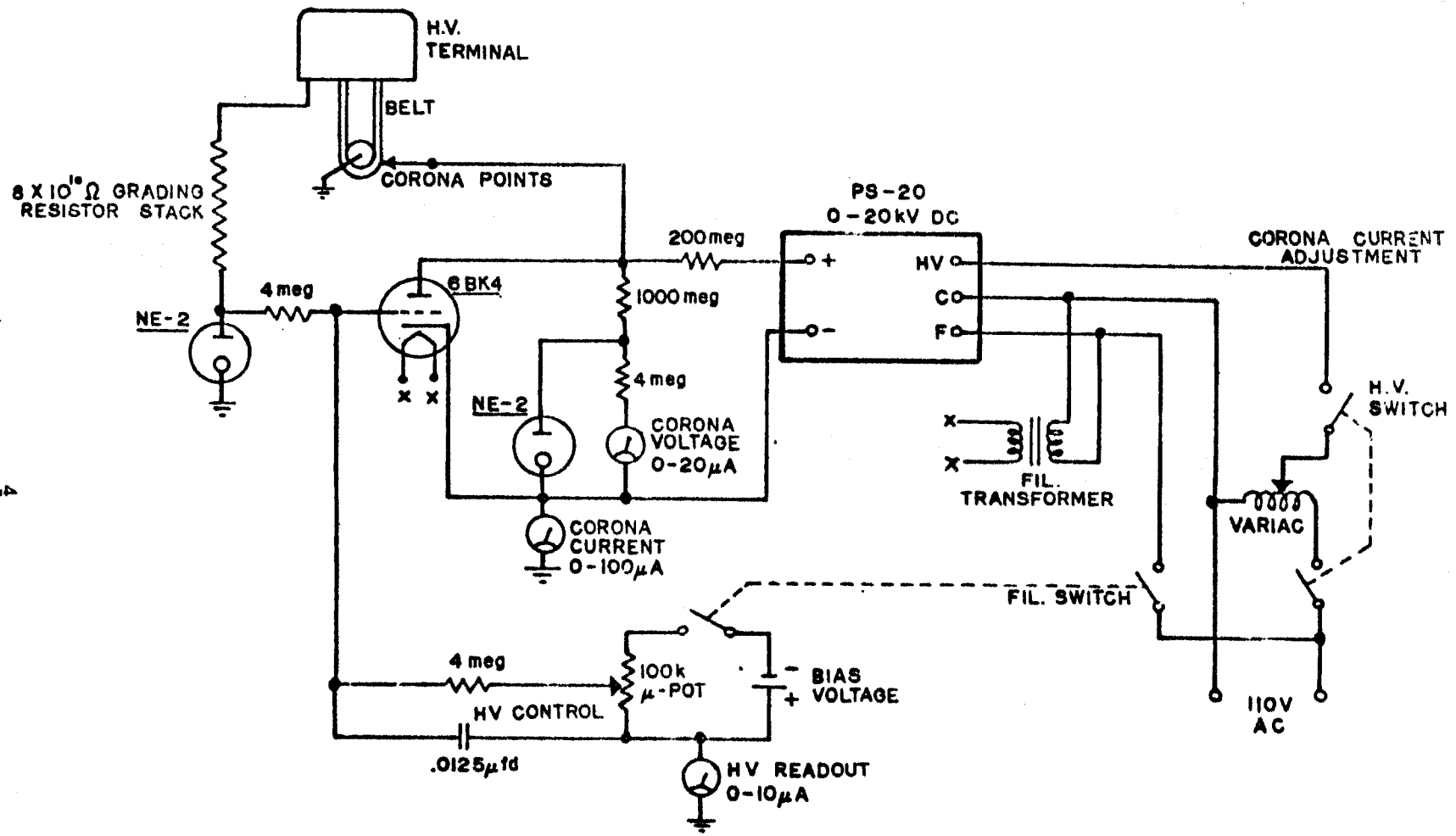

FIG. I-VAN DE GRAAFF GENERATOR VOLTAGE CONTROL CIRCUIT

over time lengths longer than a fraction of a second. Shorter duration variations are adequately filtered by the capacitance of the terminal, etc., to ground. This sort of control and stabilization circuit has provided voltage setting accuracy of ±1% and regulation to within ±2% in similar applications.

The equipotential planes, or decks, in the generator support structure, or column, are separated by glass insulators which are fastened by a special adhesive. Assembly of the column structure requires a jig to hold the pieces in place while the adhesive is cured. The jig is detailed in the drawing numbered 23049. As outlined in the Monthly Technical Report No. 4, three decks with grading resistors, etc., have been fabricated and joined for the purpose of preliminary voltage testing. The test is to check out the grading resistor assembly, which is peculiar to the new design. The assembly jig has necessarily also been fabricated. Views of the jig and the three-deck test column are shown in Fig. 2. Unfortunately, there is insufficient time to perform the actual voltage tests within the contract period. However, the assembly is available so that tests can commence immediately in the next phase of the program.

Other tests to be run on the generator will involve the whole machine in a pressure vessel by itself. The voltage, current, and regulation capabilities will be determined and the machine will be run for an extended period to assure durability. It may also be advisable to verify the voltage calibration by independent measurements with an electrostatic voltmeter.

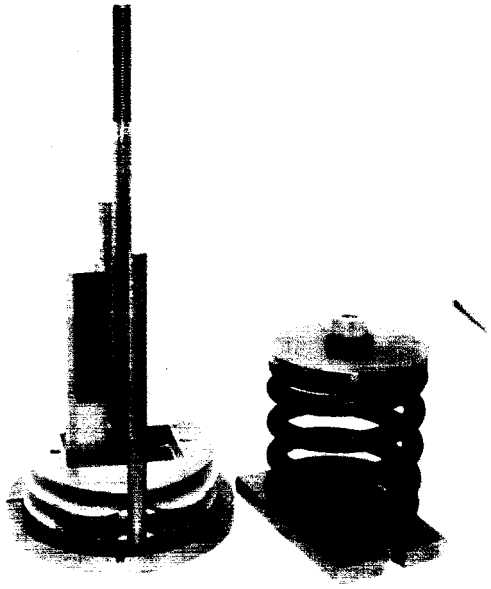

FIG. 2 - TWO VIEWS OF COLUMN ASSEMBLY JIG

I-778

3. HIGH VOLTAGE SWITCH

The prototype high voltage triggered arc switch design is given in the drawings numbered 23054-1 through 23054-13. This design is based on the most recent Ion Physics Corporation experience with similar switches at both the 150 kilovolt and 1 to 2 megavolt levels. The total of switch delay plus jitter times should be under 100 nanoseconds. As can be seen from the drawings, the damping resistor (type FFW high frequency carbon film resistor, Resistance Products Corporation) forms the suspension for the high voltage terminal of the switch. The value of resistance required to critically damp (or somewhat overdamp) the bushing discharge circuit will be determined empirically during the prototype test. The resistance can be estimated to be in the range 40 to 1000 Ω so that values in this range will be tested. The trigger gap is mounted in the ground terminal, the 50 kV trigger pulse being introduced via the conducting rod up the center. Provision has been made for mounting a short length of resistance wire on the insulating block of the ground terminal so that it comes between the terminal and the pressure vessel and is thus in the discharge path. This will serve as the pulse monitoring resistor. An appropriate pressure-to-cable bushing has been provided in the generator base plate so that the signal can be transmitted for remote display.

For test purposes, the switch will be set up in a jig and placed within the tank of a conventional 1.3 MV Van de Graaff generator in such a way that it may be used to discharge the high voltage terminal. In this application, the generator will be run at 500 kV. The switch will be fired repeatedly while delay and jitter times are measured by high speed oscilloscope photographs. Firing will be accomplished by the trigger pulse circuit described later in this report, so that trigger performance (delay and jitter) will be

measured simultaneously. The durability and reliability of the switch and trigger over a thousand or more discharge cycles will be verified under energy flow conditions closely approximating those of the ultimate application.

4. HIGH VOLTAGE BUSHING

The prototype high voltage pressure-to-vacuum bushing design is detailed in the drawings numbered 23003-1 through 23003-11. The pressure tank to contain the gas insulation is shown in Drawing No. 23002 and the port modifications for mounting the bushing-generator-switch package in an existing four-foot diameter stainless steel vacuum vessel are shown in Drawing No. 23001. The isolation grid is detailed in Drawing No. 23047 and a drift tube mockup assembly in drawings numbered 23048, 23003-5, 23003-6 and 23003-9. Castered stands to assist in the mounting and demounting of the pressure vessel and the bushing are shown in drawings numbered 23021 and 23022 respectively. The pressure vessel stand also may be used for generator removal as well.

All specifications have been met except that the bushing is slightly over 26 inches in overall length rather than 23 inches. The extra length is on the vacuum side and provides a further margin of safety against voltage breakdown along the glass insulating column while still leaving a vacuum insulation distance between opposing bushing terminations of over 14 inches which should be quite adequate. The original bushing length limit was laid down primarily to ensure that the maximum diameter of the accelerator would not exceed 8 ft 9 in., a specification which has not been altered by the change in bushing length.

The bushing test sequence will begin with d.c. conditions and proceed finally to pulsed conditions, employing the generator and switch described previously. Under d.c. conditions, bushings of similar design have provided as much as 800 kV, negative polarity, in a 10^{-7} torr vacuum environment. Previous tests have indicated no change in bushing capability from 10^{-6} torr to 10^{-7} torr, so the capability at 10^{-8} torr will be assumed

the same provided this result is verified. That the bushing will support 500 kV d.c., negative polarity, is not in doubt. The d.c. tests will actually serve only to establish the cleanliness of the bushing and tank and provide a performance base line from which the pulsed measurements may proceed.

The bushing performance under pulsed conditions is unknown and is the most important quantity to be established in the bushing test sequence. No serious difficulties are anticipated, but two unlikely possibilities must be explored. The first is the possibility that flashover or sparking in vacuum across the glass segments of the graded insulating column may occur during pulsing. This column is resistively graded for d.c. conditions, but becomes capacitively graded under pulsed conditions. The capacitive grading will not be uniform, which circumstance may result in voltage overstress across some of the glass segments. The second possibility is that a spark occurring on a bushing being discharged may, by charged particle or ultraviolet radiation emission, trigger breakdown on the adjacent bushing leading to its partial or complete discharge prematurely.

The question of sparking can be settled by simply viewing the glass column during bushing discharge. The test vessel is equipped with three viewing ports, so this presents no problem. One of these ports is in the same side of the vessel as the bushing, in the approxmate position the adjacent bushing would occupy. The induced sparking question can be settled by fitting this port with a blank-off, in which is mounted one of several existing 200 kV air-to-vacuum bushings. Fastened to the vacuum end of the bushing would be one segment of a 500 kV bushing column consisting of a metal plate (connected to the bushing conductor), a glass ring, and a metal ring connected to ground. An external 160 kV power supply can then be used to apply sufficient overvoltage across the glass ring to lead to sparking while the adjacent 500 kV bushing is at operating potential. This situation

presents the most favorable conditions for induced sparking and, again, visual observation will settle the question, reinforced with observations of generator terminal voltage behavior. Should either of the sparking possibilities prove to be a serious problem, further experiments and possibly bushing redesign would be necessary. Present test plans involve the temporary use of an existing glass insulating column assembly so that if redesign is necessary, very little will have been lost.

The one final quantity to be measured is the capacitance between opposite bushings, which is the largest of the interstage capacitances. Since this is due mainly to the drift tubes and bushing terminations, measurement can be accomplished by attaching a drift tube mockup to the plate of the 500 kV bushing section which will have been mounted on the 200 kV bushing in the previous test and inserting this assembly in the viewing port directly opposite the bushing under test. The measurement can be obtained either with a capacitance bridge or by direct observation of the induced voltage pulse during bushing discharge. The importance of the interstage capacitances is that they cause partial discharge of all bushings when any one is grounded, as explained in previous reports. If the measured capacitances are small enough that voltage sag stays within the ±5% specification, no problem exists. This is not likely; however, there are several simple expedients, involving the use of grounded shielding wires, which would probably serve to reduce the interstage capacitances to a harmless level. Even if this is not adequate, it will only be necessary to program the voltage sequence of the stages so as to compensate.

5. ELECTRONICS

A block diagram for the electronics circuitry is given in Fig. 3. There are three essential changes from the circuit concept of previous reports.

Firstly, the detector pulse simulator (P) has been moved back behind the detector preamplifier so that it serves to check out all the sequencing electronics instead of only the portion at ground potential. The obvious advantages of this arrangement require no elaboration.

Secondly, the amplified detector pulse is transmitted to ground potential by means of the coupling transformer (T) rather than a blocking capacitor. This transformer is insulated for 5 kV between primary and secondary and has a turns ratio of 15:1, providing voltage gain between the detector amplifier (A_2) and the delay generator (D). This gain is necessary because the detector amplifier output is about 1.5 V while the delay generator requires a minimum 15 V triggering signal amplitude. The transformer also provides much better isolation from pre-acceleration power supply (G_1) noise so that there is no longer a signal-to-noise ratio problem at the delay generator input. It has thus been possible to eliminate the potential divider entirely, since its purpose was reduction of the noise to a level below the delay generator triggering threshold. It is apparent that circuit performance has not been degraded in any important way by the change to a coupling transformer.

The third change which has been made is that the delay generators are now series connected rather than paralleled. Thus, only the 10-100 μsec range of each generator need be used so that range switching is eliminated, resulting in simplification of the control circuitry. Delay generator

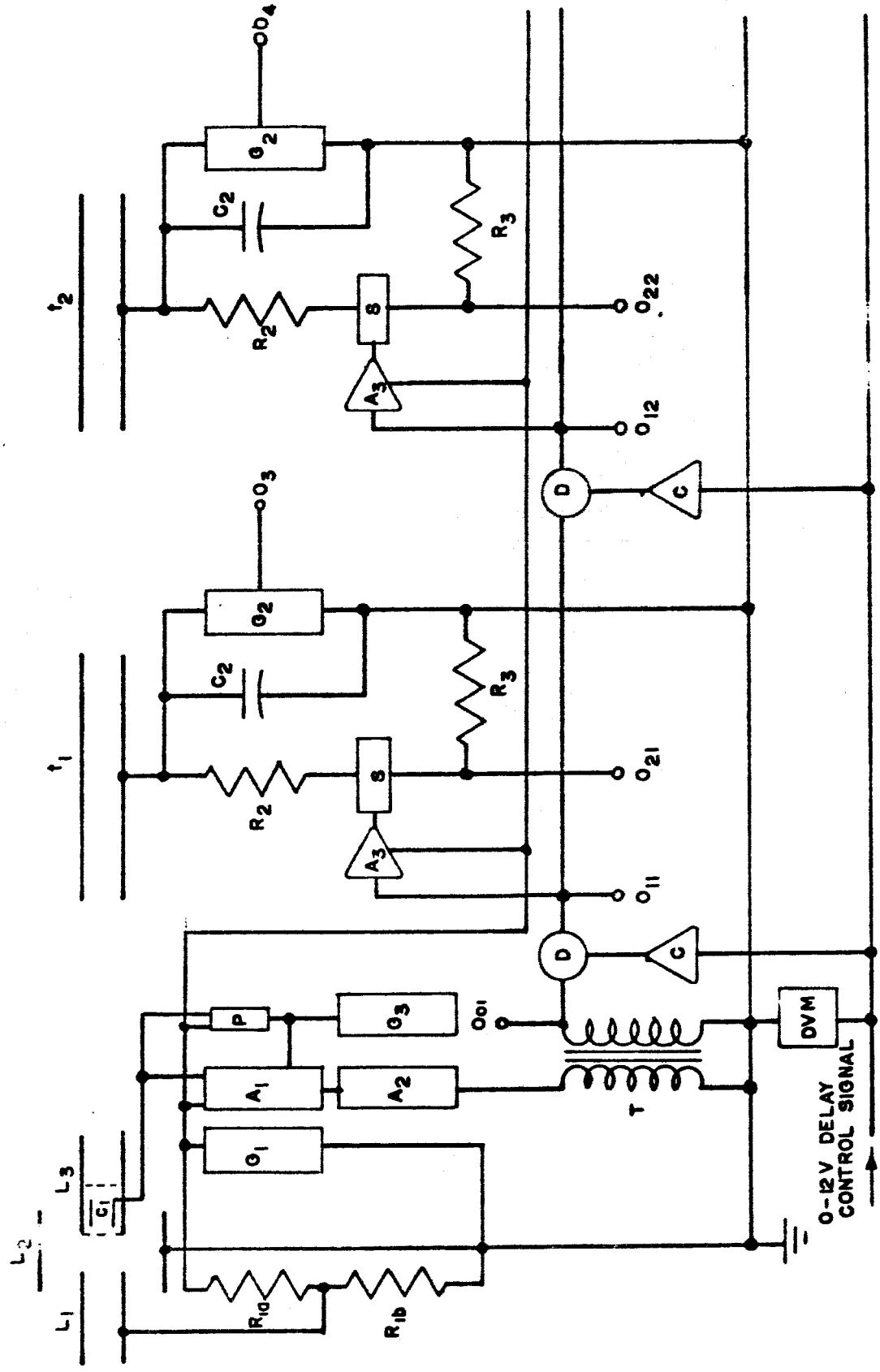

FIG. 3 - ELECTRONIC BLOCK DIAGRAM (FINAL TWO STAGES OMITTED)

Key to Figure 3

L_1, L_2, L_3	-	focusing lens elements
t_1, t_2	-	drift tubes
C_1	-	detector capacitance
C_2	-	bushing plus Van de Graaff generator capacitance to ground
R_{1a} R_{1b}	-	voltage divider for obtaining focusing
R_2	-	damping resistor; Resistance Products Corp. type FFW
R_3	-	pulse monitoring resistor; resistance wire
G_1	-	pre-acceleration voltage supply; Fluke Model 408-A
G_2	-	Van de Graaff generator
G_3	-	preamplifier power supply; Space Technology Laboratories Model 1PPS 100D
A_1	-	detector preamplifier; Space Technology Laboratories particle detector preamplifier
A_2	-	detector amplifier; 2 Teltronics Inc. model VA -20 in series
A_3	-	switch trigger amplifier; see Fig. 5
P	-	detector pulse simulator; see Fig. 4
T	-	coupling transformer; E. G. and G. TR-36
S	-	triggered arc switch
D	-	variable delay generator; Rutherford Electronics Company model A-2
C	-	delay module control circuit; see Fig. 6
DVM	-	5 digit digital voltmeter; Hughes Instruments model 5100 or equivalent
O_{10}, O_{11}, etc.	-	signal outputs for viewing timing sequence and bushing discharge signals on external oscilloscope
O_3, O_4	-	high voltage monitoring outputs

uncertainties are now additive along the accelerator, but the net effect is a reduction because the large uncertainty of the 100-1000 μsec scale (±2 μsec) is avoided. Hand computations based on the computer sequencing calculations indicate that, with some small changes in drift tube lengths, the accelerator can tolerate a delay uncertainty at each stage of +0.30 μsec or -0.25 μsec (±0.25% of full scale with up to 0.05 μsec delay generator output pulse rise time) in addition to ±1% uncertainty in the delay control signal voltage. The delay generator which has been chosen is rated as accurate to ±0.2% of full scale and will provide an output pulse with a rise time to triggering voltage (15 V) of less than 0.05 μsec. The delay control signal can be accurate to a small fraction of 1%, so that a reasonable safety margin exists on all specifications.

Most of the components involved in the block diagram are commercially available, and manufacturers' names and model numbers are provided in the Key to Fig. 3. Among the items not indicated in Fig. 3 are an isolation transformer to provide line power to the components held at preacceleration voltage, and a line voltage regulating transformer from which all the electronic components will be operated. The former is Del Electronics Corp. model AD1641 and the latter is Sola Electric Co. Solatron model 31-13-250. Circuit diagrams are provided for the three components which have had to be designed.

The pulse simulator circuit is shown in Fig. 4. It can be actuated from a station at ground potential by virtue of the isolation transformer, and provides a single pulse output of width 10 μsec, rise (and fall) time 1 μsec, and height variable from 0 to 100 μV. These conditions correspond to the fastest pulse which will be generated in practice and thus duplicate the worst conditions under which the sequencing circuitry must operate.

Figure 5 shows the switch trigger amplifier, or initiator, circuit. It converts the 50 V delay generator pulse output into a pulse rising to 50 kV in less than 1 μsec.

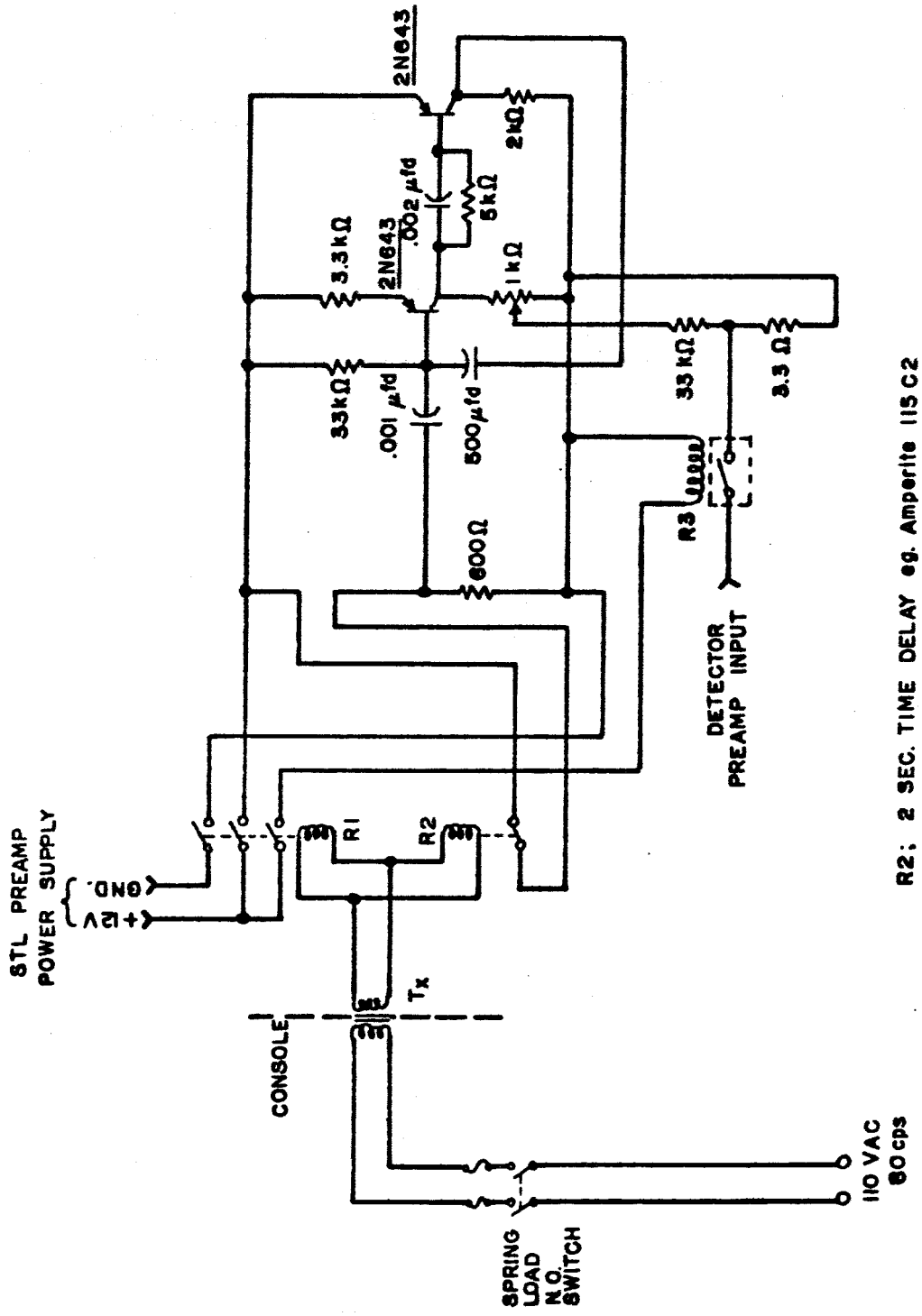

R2; 2 SEC. TIME DELAY eg. Amperite 115 C2

R3; >100 AMP TURNS; G.E. CR 144 R1 REED SWITCH (1.5 pF. max.; $5 \times 10^{11}\Omega$ min)

Tx; 115 VAC / 115 VAC 5kV INSULATION

FIG. 4 - PULSE SIMULATOR CIRCUIT

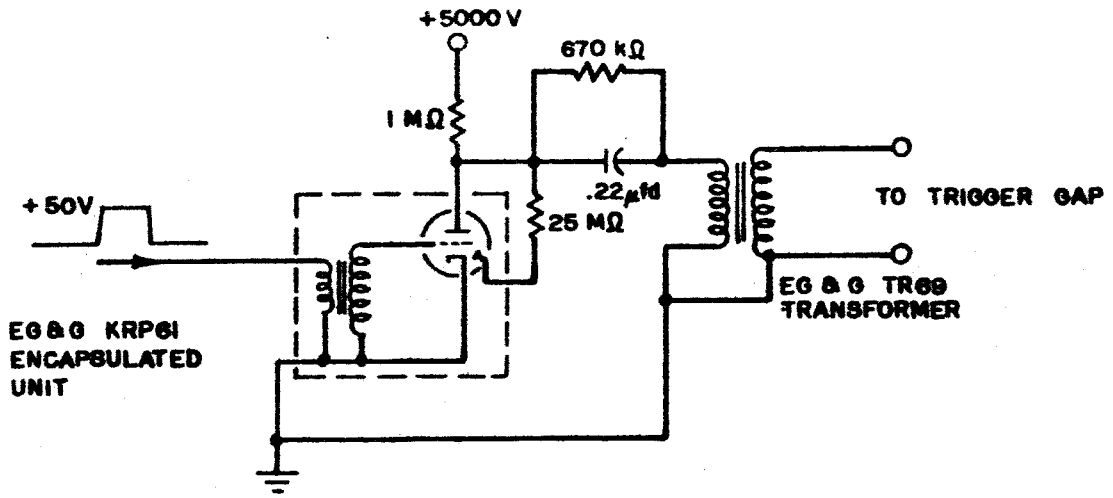

FIG. 5 – SWITCH TRIGGER AMPLIFIER CIRCUIT

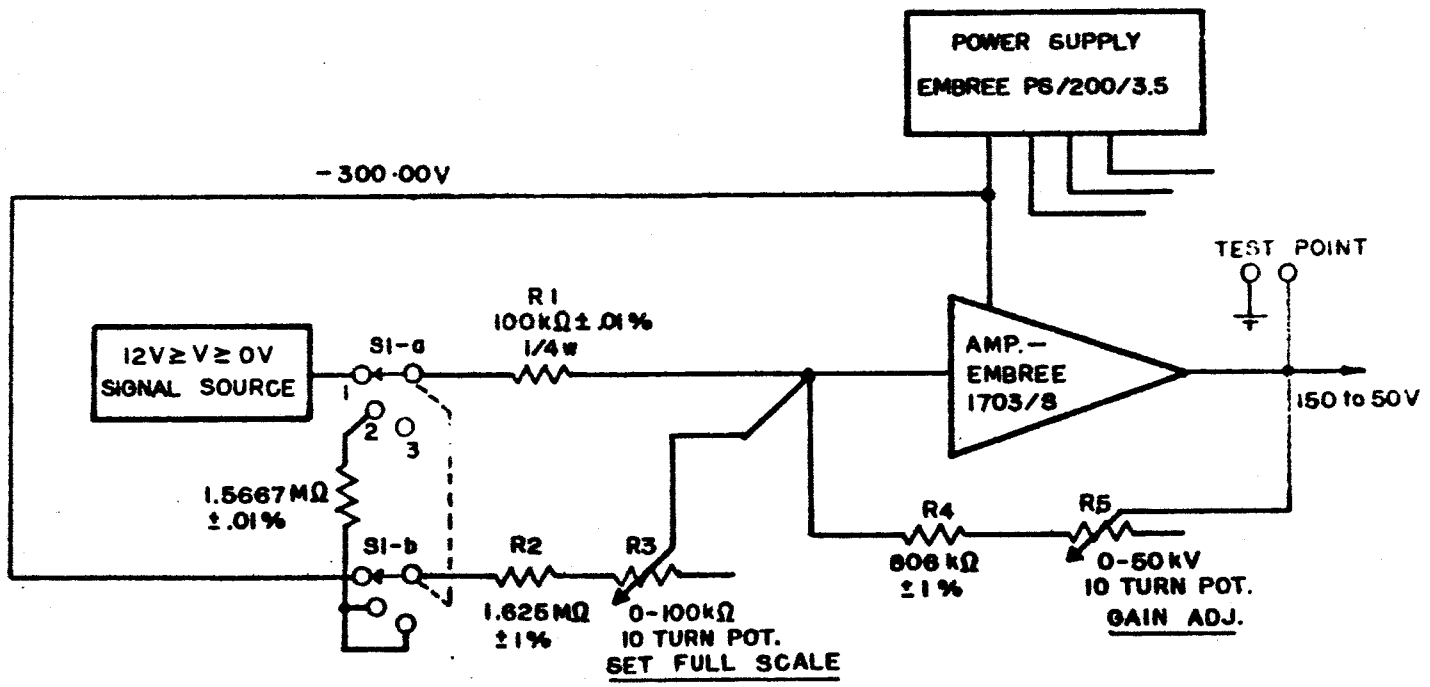

FIG. 6 – DELAY MODULE CONTROL CIRCUIT

Figure 6 shows the delay module control circuit. The delay generator may be controlled by an applied voltage, 150 V corresponding to zero delay and 50 V to full scale delay. With the delay control signal at 0 V, the Set Full Scale control is adjusted to produce 150 V output, and with the signal at 12 V, the Gain Adjust control can be set to produce any desired maximum delay in the operating range. The Gain Adjust controls thus allow the setting of the delay modules in a sequence of ratios while the delay control signal provides for ganged control of all four modules simultaneously, thus setting the time scale appropriate for any particular charge-to-mass ratio being accelerated. The delay control signal setting (which is inversely proportional to the square root of the charge-to-mass ratio) is monitored by a digital voltmeter (see Fig. 3), which is also used in calibration of the delay module control circuits. The control signal can be derived from the power supply of Fig. 6 by means of a potentiometer and variable resistor combination (not shown). It should be noted that one of these power supplies is sufficient for driving all of the delay module controls so that this component need not be replicated at each stage.

Tests of the electronics are chiefly a matter of calibration and verification of component specifications and determination of system performance by means of a high speed oscilloscope (pulse rise times, delay accuracy, etc.). Reliability can be assessed by observing system performance over a great number of acceleration cycles using the pulse simulator to provide triggering.

6. AUTOMATIC CONTROL SYSTEM PRELIMINARY DESIGN

A block diagram for an automatic control system for the microparticle accelerator is given in Fig. 7. This system produces a delay control signal output directly from the drive and test frequency signals of the ARC microparticle source, as well as giving direct indication of particle charge-to-mass ratio.

A pair of independent 0-10 volt control signals regulates a pair of linear voltage-to-frequency converters (VTF) to provide source drive and test signals. The control signals are also multiplied in an analogue multiply module (M) and the result scaled by an amplifier (A) and measured by a digital voltmeter (DVM). Since the charge-to-mass ratio is proportional to the product of the drive and test frequencies, the amplifier gain can be adjusted so that the voltmeter indicates the charge-to-mass ratio (or perhaps, more conveniently, one tenth of this ratio) directly. The accuracy of the indication could be a fraction of a percent, taking the control signals to be perfectly accurate. The control signals would also drive an analogue computer involving square root and divide modules (SR, D) to produce an output inversely proportional to the square root of the product of the signals, hence directly proportional to the accelerator time scale. If the output signal magnitude is appropriately adjusted, it could be used as the delay control signal. As noted in Section 5, an accuracy in this signal of $\pm$ 1% is tolerable. The computing circuit of Fig. 7 is not the simplest conceivable, but gives a more accurate result which is just sufficient for the requirements.

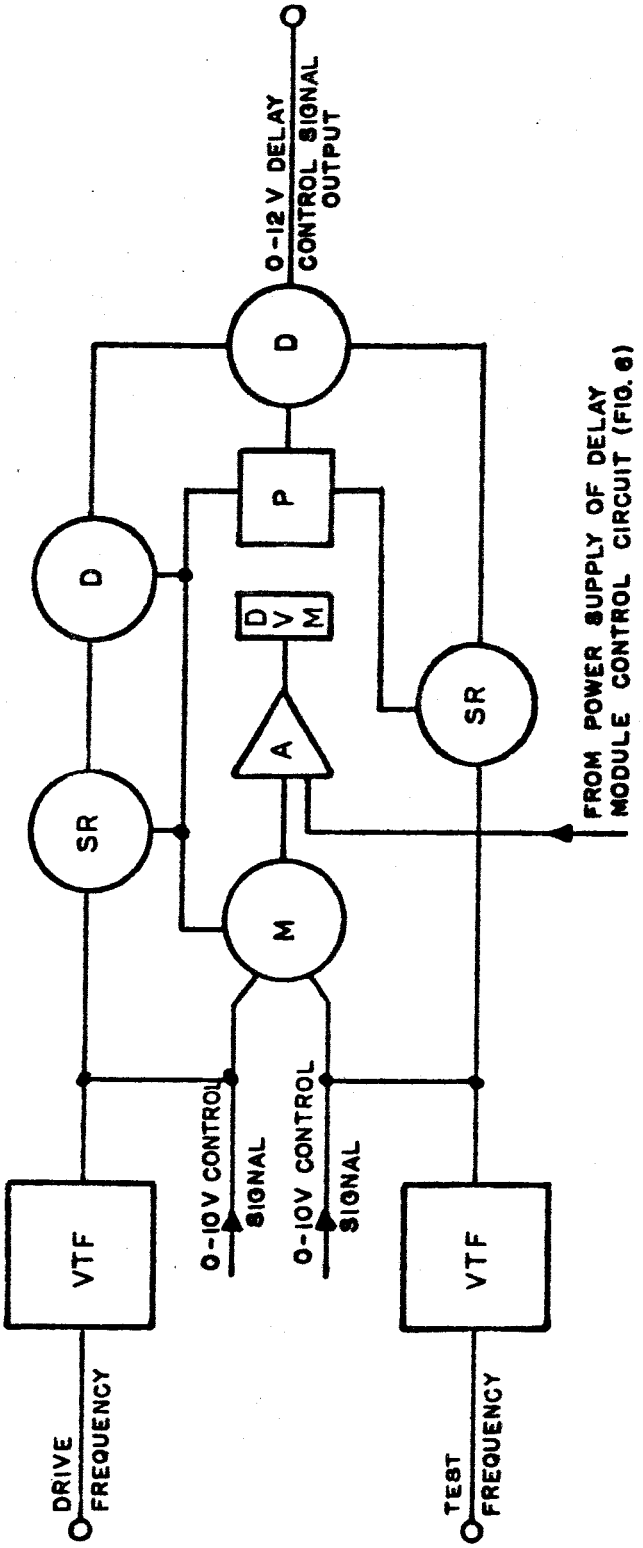

FIG. 7 – AUTOMATIC CONTROL SYSTEM BLOCK DIAGRAM

Key to Figure 7

VTF	-	voltage-to-frequency converter; see Figs. 8, 9	
DVM	-	digital voltmeter	
A	-	amplifier	
M	-	analogue multiply module	e.g., Consolidated Electrodynamics (Devar Kinetics Div.) Model 19-302 in appropriate connections
SR	-	analogue square root module	
D	-	analogue divide module	
P	-	analogue module power supplies; e.g., Consolidated Electrodynamics models 19-601 and 19-603	

The voltage-to-frequency converters could be electronic or electromechanical. In either case, conversion accuracy of a fraction of a percent is achievable. A block diagram illustrating the electromechanical approach is given in Fig. 8. A servo motor (M) simultaneously drives an accurate oscillator (O), having a linear control characteristic, and a potentiometer in one arm of a bridge circuit (B). The control signal drives another arm of the bridge. Bridge imbalance is sensed by the amplifier (A) which controls a sensitive relay (R) which in turn controls the servo motor in such a way as to eliminate the imbalance. In this way, the oscillator output frequency can be made proportional to the control signal voltage.

In the electronic approach illustrated in Fig. 9, an electronic voltage-to-frequency converter (C) provides a square wave output with a frequency proportional to the control signal voltage. The harmonics of the output wave are attenuated in an R-C filter (F) and the filter output is passed to the amplifier (A). This is equipped with an automatic gain control circuit so that its output amplitude remains reasonably constant even though the filter output drops as the frequency is increased.

The electronic converter is less expensive that the servo controlled oscillator, but can never be as nearly free of harmonics. A decision between the two must be based on a clearer understanding of the ARC microparticle source requirements, and will therefore be deferred to a later time.

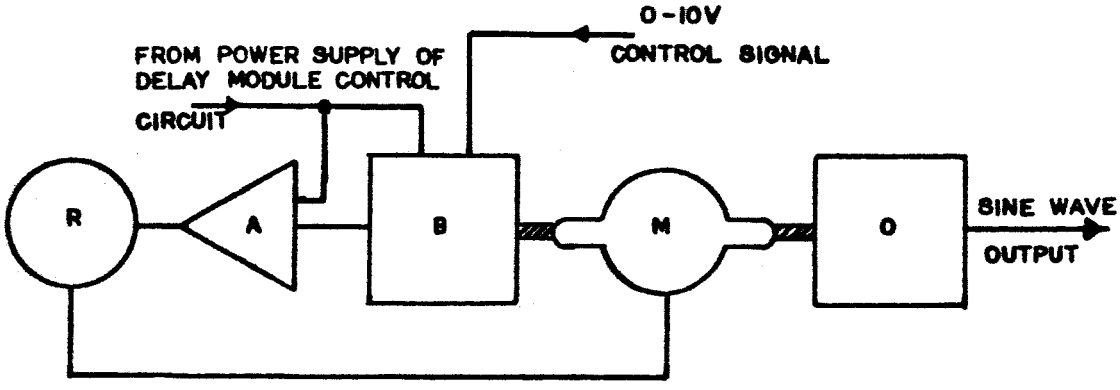

O – HIGHLY ACCURATE OSCILLATOR (GENERAL RADIO 1107A)

M – SERVO MOTOR

B – BRIDGE CIRCUIT

A – AMPLIFIER

R – MICROPOSITIONER RELAY

FIG. 8–SERVO CONTROLLED OSCILLATOR BLOCK DIAGRAM

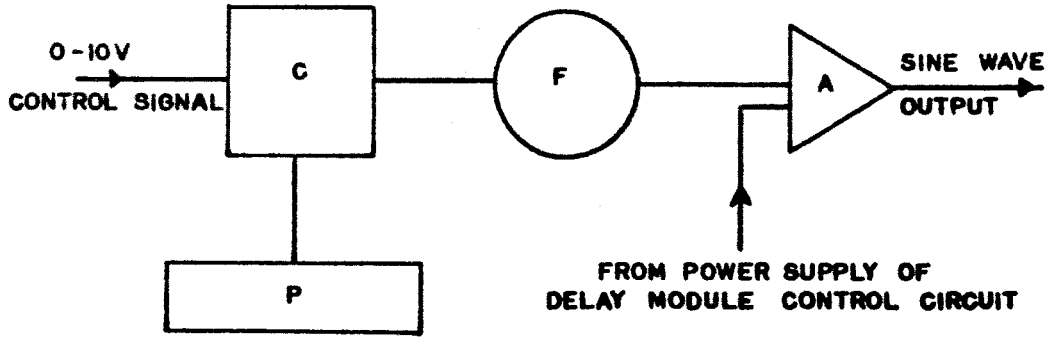

C – ELECTRONIC VOLTAGE-TO-FREQUENCY CONVERTER (VIDAR 211B)

P – CONVERTER POWER SUPPLY (VIDAR 101)

F – R-C FILTER

A – AMPLIFIER

FIG. 9-ELECTRONIC VOLTAGE-TO-FREQUENCY CONVERTER BLOCK DIAGRAM

7. PROTOTYPE SYSTEM TEST

The prototype system will be put through the acceleration cycle repeatedly, using the pulse simulator, to assess the reliability of operation. Performance can be monitored by high speed oscilloscope and the built-in instruments. This test should establish what recalibration and/or servicing periods for the various components are consistent with the maintenance of high accelerator performance reliability and minimum down time.

As soon as system performance is firmly established, a reapportionment of drift tube lengths will be made, in line with the comments in Section 5, and recalculation of the accelerator timing sequence will be undertaken, using the computer program previously devised. In this way, an optimum distribution of safety margin among the stages can be realized. No increase in acceleration path length is involved in this reapportionment.